

# Theory of the Josephson Junction Laser

Steven H. Simon<sup>1</sup> and Nigel R. Cooper<sup>2</sup>

<sup>1</sup>*Rudolf Peierls Centre, Oxford University, OX1 3NP, United Kingdom*

<sup>2</sup>*T.C.M. Group, Cavendish Laboratory, J.J. Thomson Avenue, Cambridge, CB3 0HE, United Kingdom*

(Dated: June 30, 2022)

We develop an analytic theory for the recently demonstrated Josephson Junction laser (Science **355**, 939, 2017). By working in the time-domain representation (rather than the frequency-domain) a single non-linear equation is obtained for the dynamics of the device, which is fully solvable in some regimes of operation. The nonlinear drive is seen to lead to mode-locked output, with a period set by the round-trip time of the resonant cavity.

A remarkable recent experiment by Cassidy *et al.*[1] demonstrated the operation of a Josephson junction laser. The device is a resonator cavity (a half-wave coplanar waveguide) of fundamental frequency  $\omega_0$  with a Josephson junction coupled to one end of the cavity near an antinode of the cavity electric field and biased with a DC voltage  $V$ . While this general experimental configuration has been used in numerous experiments previously (see for example, [2–4]), the work by Cassidy *et al.* observes phenomena that have many features of lasing in a new and unexplored regime.

In [1], a simple theory, based on the work of [5], was proposed comprising a transmission line cavity coupled to a Josephson junction and biased with a DC voltage  $V$ . The equations of motion for the amplitude  $\phi_n$  of the  $n^{\text{th}}$  mode of the cavity are given by

$$\ddot{\phi}_n = -\omega_n^2 \phi_n - 2\gamma \dot{\phi}_n + \alpha_n \lambda \sin \left[ Vt + \sum_n \alpha_n \phi_n \right] \quad (1)$$

with  $n = 1, 2, \dots$ . (See Supplementary Material of [1], and also the Supplementary Material of the current paper[6] for a rederivation.) Here,  $\omega_n$  is the frequency of the  $n^{\text{th}}$  mode,  $\lambda = 2E_J/C$  where  $E_J$  is the Josephson energy and  $C$  is the total capacitance of the waveguide (capacitance per unit length times length). The parameter  $\gamma$  is the damping, and the parameters  $\alpha_n$  are the couplings of the modes to the junction. Note that we have set  $2e/\hbar$  to unity. This describes a set of driven and damped harmonic oscillators, where the driving force is the current injection from the junction. For an ideal waveguide  $\omega_n = n\omega_0$ ,  $\alpha_n = 1$ , and  $\gamma = 0$ . However, these assumptions are not crucial.

In [1] lasing was found only when many modes of the junction were considered ( $\alpha_n$  nonzero and approximately unity for  $n$  up to about 20), thus giving a system of many simultaneous differential equations. We will transform this problem so that analysis is relatively simple and the physics of the laser will become transparent.

The key to our analysis is to work in a real-time picture rather than in terms of the individual modes of the cavity. We find solutions in which the many modes of the cavity coherently combine to form discrete pulses which reflect

back and forth in the cavity, as in a mode-locked laser, and which have a natural description in the time domain.

We first think about the response of each mode to a drive at the position of the junction. We denote the retarded Green's function of the  $n^{\text{th}}$  simple harmonic oscillator as  $G_n(t)$ , which in the absence of damping takes the simple form  $G_n^0(t) = \Theta(t) \sin(\omega_n t)/\omega_n$  with  $\Theta$  the step function. (The superscript  $0$  indicates no loss.) Since all of the modes couple to the same source, we group them all together by defining

$$\Psi = \sum_n \alpha_n \phi_n. \quad (2)$$

The voltage across the junction is simply  $V_J = V + \dot{\Psi}$ . The retarded Green's function for  $\Psi$  is then just

$$K(t) = \sum_n \alpha_n^2 G_n(t)$$

The dynamics of the system may then be recast as a single equation

$$\Psi(t) = \lambda \int_{-\infty}^t dt' K(t-t') \sin[Vt' + \Psi(t')] \quad (3)$$

This is a highly nonlinear equation. As is often the case with such equations, many solutions may exist and solutions may depend on initial conditions as well.

To understand the form of the kernel  $K(t)$ , consider first the ideal case of no damping  $\gamma = 0$  with  $\omega_n = n\omega_0$  and  $\alpha_n = 1$ . Then  $K$  has a sawtooth form  $K^0(t) = (1/2)[T/2 - (t \bmod T)]$  where  $T = 2\pi/\omega_0$  is the “round-trip” time of the cavity. Once one adds damping, with  $\gamma \ll \omega_0$ , to a very good approximation the response is the decaying sawtooth (See also Supplementary Material[6])

$$K(t) = e^{-\gamma t} K^0(t). \quad (4)$$

It is important to note that even if one adds randomness to the frequencies  $\omega_n$  and to the couplings  $\alpha_n$  the general sawtooth form persists (See also Supplementary Material[6]). The sudden step is simply a result of the fixed time delay associated with the round-trip time of the cavity. In cases where the waveguide has dispersion

(i.e. the mode spacing varies smoothly with  $n$ ), the round trip time may depend on the shape of the wavepacket.

Note that in the case where  $\Psi \ll 1$ , which results from either small  $\lambda T^2$  or large  $\gamma T$ , we can treat Eq. 3 perturbatively. At zeroth order, we drop  $\Psi$  on the right hand side and have a simple integral on the right. For example, in the case of large  $\gamma T$ , one obtains  $\Psi^{(0)}(t) = (\lambda T/4\gamma) \sin Vt$  with the superscript here meaning at zeroth order. We can then plug this  $\Psi^{(0)}$  into the right hand side of Eq. 3 and again perform the integral, to obtain an improved approximation  $\Psi^{(1)}$  at first order, and so forth. It is easy to establish that this procedure only ever generates harmonics of the frequency  $V$  at long times, i.e., the time period of oscillation is  $2\pi/V$ . At large  $\gamma T$ , this arises because the function  $K(t)$  has decayed to almost zero before reaching  $T$ , so its sawtooth form has been lost and the time period  $T$  forgotten.

However, for small  $\gamma T$  (believed to be appropriate for the experiment[1]) with large  $\lambda T^2$  there is a different type of solution where the oscillation period will instead be  $T$ . Much of the remainder of this paper will explore this possibility.

Using the form of Eqs. 4, we can transform Eq. 3 to

$$\Psi(t) = \Psi(t-T)e^{-\gamma T} + \lambda \int_{t-T}^t dt' K(t-t') \sin[Vt' + \Psi(t')] \quad (5)$$

The first term on the right here represents the integration from  $-\infty$  to  $t-T$ . The interpretation of this equation is that a signal  $\Psi(t-T)$  has gone down the waveguide and returned after time  $T$  having decayed by  $e^{-\gamma T}$ . The resulting signal  $\Psi(t)$  is this decayed signal plus the result of driving by the Josephson junction during the period  $t-T$  to  $t$ .

Let us consider first the special case of  $\gamma = 0$  and a voltage  $V$  that is commensurate with the period  $T$ . I.e., we set  $V = V_m = 2\pi m/T$  for some integer  $m$ . Looking for a periodic solution we set  $\Psi(t-T) = \Psi(t)$ . Eq. 5, can then be satisfied by having the sin be a constant since the integral of  $K^0$  over a period vanishes. Thus we set

$$\Psi(t) \bmod 2\pi = -V_m t + \beta \quad (6)$$

for some constant  $\beta$ . The right hand side is a linearly decreasing function of time, but can be made periodic by inserting  $m$  phase slips of  $2\pi$  during the cycle (i.e., making it a sawtooth). The phase slips may be at any point in the cycle of time  $T$ , although they need to be the same from one cycle to the next to ensure  $T$ -periodicity. This analytic solution matches numerical solutions for small  $\gamma$  and commensurate  $V$  quite well as shown, for example, in Fig. 1. This form of solution remains valid for any form of  $K^0(t)$  so long as its integral over a period vanishes. In particular this will be true for any parameters  $\alpha_n$  we choose in Eq. 2 (See also Supplementary Material[6]).

The power absorbed by the waveguide is  $P = (V_J - V)I = \dot{\Psi}E_J \sin(Vt + \Psi)$ . Here  $V_J - V = \dot{\Psi}$  is the voltage

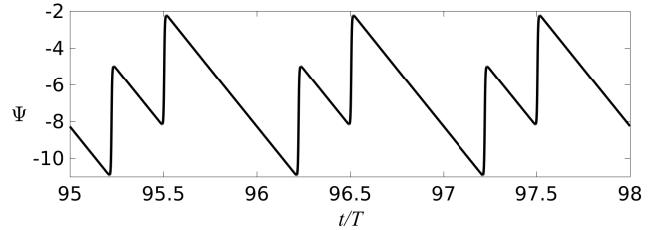


FIG. 1. Numerical form of  $\Psi(t)$  obtained by integration of Eq. 5 for parameters  $V = 2, \gamma = .01, \lambda = 6$  in units where  $T = 2\pi$  so  $\omega_0 = 1$ . The waveform has constant negative slope with discrete steps of  $2\pi$ . Note that the two steps within each cycle are not equally spaced but the pattern is periodic with period  $T$ .

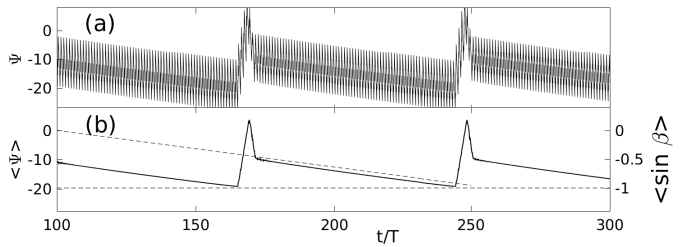


FIG. 2. Numerical form of  $\Psi(t)$  obtained by integration of Eq. 5 for parameters  $V = 4.02, \gamma = .05, \lambda = 12$  in units where  $T = 2\pi$ . (a) Oscillations of  $\Psi$  over several hundred periods. (b) Plot of  $\langle \Psi \rangle$  which is  $\Psi$  averaged over a period  $T$  with vertical scale on the left, and also a plot of  $\langle \sin \beta \rangle$  which is  $\sin[Vt + \Psi]$  averaged over a period  $T$  with vertical scale on the right. The two vertical scales are in ratio of  $\lambda T^2/24$  as predicted by Eq. 11. The two curves ( $\langle \sin \beta \rangle$  and  $\langle \Psi \rangle$ ) overlay so precisely that they are not both visible on this figure. The diagonal dashed line is the predicted slope  $-\delta Vt$  as discussed in the text. Note that when  $\sin \beta$  reaches  $-1$  (the horizontal dashed line) the form of solution changes for a short period of time.

from the injection point of the waveguide (the connection of the Josephson junction to the waveguide) to the ground. Thus the energy absorbed by the waveguide per cycle is

$$E_{\text{absorbed}} = \int_{t-T}^t dt' E_J \dot{\Psi}(t') \sin(Vt' + \Psi(t')) \quad (7)$$

$$= -VTE_J \langle \sin \beta \rangle \quad (8)$$

where we have integrated by parts (and disregarded boundary terms assuming a periodic or almost periodic solution), and the brackets indicate the average of the sin over the cycle.

If there is a damping  $\gamma > 0$  then there will be a loss per cycle of  $E_{\text{stored}}(1 - e^{-2\gamma T})$  where  $E_{\text{stored}}$  is the stored energy in the waveguide. For a steady state, we thus require that  $E_{\text{stored}} = -VE_J \langle \sin \beta \rangle / (2\gamma)$ , for small  $\gamma T$ . From this we can estimate the maximum waveguide volt-

age (maximum  $\dot{\Psi}$ ).

Since  $\Psi$  is basically a sum of sawtooth waves, we consider a sawtooth with a single  $2\pi$  step which has Fourier modes  $\sin(2\pi nt/T)$  of amplitude  $2/n$ . To determine the energy stored in each of these modes, refer back to Eq. 1 and note that the energy stored in a single oscillator is[7]

$$E_{\text{stored}} = \frac{C}{4} V_{\text{max}}^2 = \frac{C}{4} (\dot{\phi}_n)^2 = \frac{C}{4} \left( \frac{2\pi n}{T} \frac{2}{n} \right)^2 = \frac{4\pi^2 C}{T^2}$$

To represent the finite slope of the steps, we cut off the higher Fourier modes by using instead Fourier modes of amplitude  $(2/n)f_n$  where  $f_n$  is a some cutoff function which is unity at small  $n$  and decays for large  $n$ . The total energy stored is then  $E_{\text{stored}} = (4\pi^2 C/T^2) \sum_n f_n^2$  whereas the maximum value of the voltage will be  $V_{\text{max}} = \dot{\Psi}_{\text{max}} = (4\pi/T) \sum_n f_n$ . Given that there are  $m = VT/(2\pi)$  phase slips per cycle we add together all the energy in all of these pulses to get  $E_{\text{stored}} = \xi C V V_{\text{max}}/2$  where  $\xi = \sum f_n^2 / \sum_n f_n$ . For  $f_n$  chosen as a sharp cutoff,  $\xi = 1$  whereas for an exponential cutoff  $f_n = e^{-an}$  instead we obtain  $\xi = 1/2$ . Setting the energy stored to  $-VE_J \langle \sin \beta \rangle / (2\gamma)$  with  $\lambda = 2E_J/C$  we obtain the result

$$|\dot{\Psi}_{\text{max}}| = |V_{\text{max}}| = \frac{\lambda}{2\xi\gamma} |\langle \sin \beta \rangle| \quad (9)$$

with  $\xi$  the unknown constant of order unity. Numerically we find that this formula holds with  $1/2 \lesssim \xi < 1$  whenever the solution has near to  $T$ -periodicity.

With this maximum value of  $\dot{\Psi}$  the sharp steps of  $\Psi$  occur over a time-scale  $\delta t \approx 2\pi(2\xi\gamma)/(\lambda|\langle \sin \beta \rangle|)$ . During this time the argument of the sin wraps by  $2\pi$  and  $\sin[Vt + \Psi]$  goes smoothly from  $\langle \sin \beta \rangle$  to  $-1$  to  $+1$  and then back to  $\langle \sin \beta \rangle$ . The total area under this spike should then be roughly  $-2\langle \sin \beta \rangle \delta t \approx 4\pi\gamma/\lambda$ . (If  $\langle \sin \beta \rangle = -1$  then it has to go all the way from  $-1$  to  $1$  giving a height of  $2$  whereas if  $\langle \sin \beta \rangle = 0$  then the spike goes symmetrically up to  $1$  and down to  $-1$  having net zero area.) Thus we can approximate

$$\sin[Vt + \Psi(t)] = \langle \sin \beta \rangle + \sum_j (4\pi\gamma/\lambda) \delta(t - t_j) \quad (10)$$

where  $t_j$  are the particular times when the sawtooth steps occur. This can then be plugged into Eq. 3 and integrated. The second term is responsible for producing the sawtooth steps in  $\Psi$  since it is being integrated with the sawtooth function  $K$ . Note that the coefficient of the delta function in Eq. 10 is exactly right to produce steps of size  $2\pi$  in  $\Psi$ . On the other hand, when we integrate Eq. 10 in Eq. 3, using  $\int_{-\infty}^t dt' K(t-t') = T^2/24$ , the first term gives the relationship

$$\langle \Psi \rangle = \lambda T^2 \langle \sin \beta \rangle / 24 \quad (11)$$

where again the brackets mean an average over a full cycle. This relationship is very accurately confirmed numerically, not only for the case of commensurate voltage

that we have focussed on so far, but also more generally, as shown in Fig. 2b.

We can now consider the case where  $V$  deviates from being commensurate with the period  $T$ . We write  $V = V_m + \delta V$  where  $T\delta V \ll 2\pi$ . We propose a solution of the form of Eq. 6 with  $V_m$  still commensurate and now  $\beta = -\delta V t$  is a slow function of time. We again assume there are  $m$  phase slips of  $2\pi$  per period and that they will occur at the same points in each cycle. However now  $\Psi$  is no longer periodic in  $T$  but rather shifts by  $-\delta VT$  each cycle as seen in Fig. 2a. The frequency of oscillation, however, remains  $\omega_0 = 2\pi/T$  very accurately.

Note that since  $|\sin \beta|$  cannot exceed 1, the form of solution must change after a time period  $\sim \lambda T^2 / (48\delta V)$  as shown in the figure, before it locks back into quasi-periodic behavior.

A few comments about the numerical solution of Eq. 5. For small  $\gamma T$ , the  $T$ -periodic solution seems to be fairly stable. As  $\gamma$  increases, even for  $\delta V = 0$  (commensurate driving),  $\beta$  does change slowly as a function of time, with a  $\dot{\beta}$  that appears to be proportional to  $\gamma^2/(V\lambda^2)$ . Also, for small  $\gamma$ , as  $|\delta V|$  gets larger (i.e., for  $V$  not very close to an integer multiple of  $2\pi/T$ ), the assumption of small  $T\delta V$  breaks down and the near-periodicity of the solution from one cycle to the next becomes imperfect. We also note that for  $\delta V$  small and negative a solution with  $\Psi$  having the periodicity of  $2\pi/V$  rather than  $T$  is fairly stable for  $\gamma$  not too small. We find numerically that for  $|\delta V| \gtrsim \gamma T$  the numerical solution reliably switches back to  $T$ -periodicity.

In the actual experiment[1], the cavity  $Q$  factor ( $\sim 1000$ ) is mostly limited by the shunt conductance  $G$  of the Josephson junction rather than the loss of the waveguide. This conductance can be added into Eq. 3 by adding a shunt current  $G(V + \dot{\Psi})$  to the Josephson current  $E_J \sin[Vt + \Psi]$ . For small enough shunt conductance this does not significantly change the resulting dynamics.

While the  $Q$ -factors for the numerical results shown in Fig. 1 and 2 are smaller than that of the experiment (and also  $\lambda$  is larger and  $V$  is smaller than the experiment), we find that numerical solutions using parameters close to those of the experiment show similar results to those shown here (See Supplementary Material[6] for examples).

Many of the qualitative features of the Josephson junction laser also appear in other nonlinear dynamical systems, perhaps the most familiar of which are musical instruments. A wide variety of sustained-tone musical instruments can be viewed as consisting of a linear resonator (e.g. violin string or organ pipe) which is subjected to a nonlinear drive (the violin bow, or organ reed). The nonlinearity of the drive establishes mode-locked oscillations of the linear resonator, leading to output at a fundamental and its pure harmonics even in situations in which the linear resonator itself is anharmonic[8]. For the same reason, the oscillations of the Josephson junc-

tion laser are insensitive to anharmonicities in the waveguide. Another closely related system is provided by the Gunn oscillator, where the negative differential conductance provides a nonlinear drive of a microwave cavity, leading to stable oscillations with similar mode-locked characteristics[9].

Our description of the Josephson junction laser has been entirely classical, since the Josephson phase is treated as a classical dynamical variable. Quantum behaviour is encoded in the uncertainty relation,  $\Delta N \Delta \Psi \geq 1/2$ , with  $\Delta N$  the number of Cooper pairs and  $\Psi$  the phase across the junction. Setting  $\Delta N = C \Delta V_J / (2e)$ , with  $C$  the total capacitance of the stripline, and working in terms of the relevant dimensionless voltage  $\tilde{V}_J \equiv 2eV_J / (\hbar\omega_0)$ , this becomes  $\Delta \tilde{V}_J \Delta \Psi \geq 4(e^2/h)Z_0$  where  $Z_0 \equiv \sqrt{L/C}$  is the impedance of the stripline. For the parameters of the experiments[1], this is  $\Delta \tilde{V}_J \Delta \Psi \geq 0.01$ , showing that quantum effects are expected to be small in the regimes of laser operation, with  $\tilde{V}_J$  and  $\Psi$  both of order unity or more. While one may wonder to what extent it is appropriate to call a classical system a laser, we note that it has long been understood that the essential physics of a laser is recovered in classical physics[10] and the operation of a free-electron laser is well-described by classical physics[11, 12]. The stimulated emission into the cavity is fully accounted for by a classical description of the (nonlinear) drive.

In summary we have presented an analytic framework for analysis of the Josephson Junction laser device. The presence of a non-linear element coupled to a cavity gives mode-locked emission at the round-trip time of the cavity at least in some regimes. Our time-domain framework greatly simplifies both numerical and analytic work and should aid further development of this field.

**Acknowledgements:** SHS is grateful to Lucas Casparis and the QDev journal club for introducing him in this problem. SHS has been supported by the Niels

Bohr International Academy, the Simons foundation, and EPSRC Grants EP/I031014/1 and EP/N01930X/1. NRC is supported by EPSRC Grants EP/P034616/1 and EP/K030094/1.

- 
- [1] M. C. Cassidy, A. Bruno, S. Rubbert, M. Irfan, J. Kammhuber, R. N. Schouten, A. R. Akhmerov, and L. P. Kouwenhoven, *Science* **355**, 939 (2017), <http://science.sciencemag.org/content/355/6328/939.full.pdf>.
  - [2] M. Hofheinz, F. Portier, Q. Baudouin, P. Joyez, D. Vion, P. Bertet, P. Roche, and D. Esteve, *Phys. Rev. Lett.* **106**, 217005 (2011).
  - [3] C. M. Wilson, G. Johansson, A. Pourkabirian, M. Simoen, J. R. Johansson, T. Duty, F. Nori, and P. Delsing, *Nature* **479**, 376 (2011).
  - [4] F. Chen, A. J. Sirois, R. W. Simmonds, and A. J. Rimberg, *Applied Physics Letters* **98**, 132509 (2011), <http://dx.doi.org/10.1063/1.3573824>.
  - [5] S. Meister, M. Mecklenburg, V. Gramich, J. T. Stockburger, J. Ankerhold, and B. Kubala, *Phys. Rev. B* **92**, 174532 (2015).
  - [6] S. H. Simon and N. R. Cooper, *Supplemental Material* (2017).
  - [7] Because the spatial form of the voltage is  $V_n(x) = V_n \cos(2\pi nx/\ell)$ , the total energy stored is half of the usual  $CV^2/2$ . See *Supplemental Material*[6].
  - [8] N. H. Fletcher, *Reports on Progress in Physics* **62**, 723 (1999).
  - [9] W.-C. Tsai, F. J. Rosenbaum, and L. A. MacKenzie, *IEEE Transactions on Microwave Theory and Techniques* **18**, 808 (1970).
  - [10] M. Borenstein and W. E. Lamb, *Phys. Rev. A* **5**, 1298 (1972).
  - [11] F. Hopf, P. Meystre, M. Scully, and W. Louisell, *Optics Communications* **18**, 413 (1976).
  - [12] E. Saldin, E. Schneidmiller, and M. Yurkov, *The Physics of Free Electron Lasers* (Springer, 2000).

## Supplemental Materials: Theory of the Josephson Junction Laser

### Supp. 1: Derivation of Eq. 1

Although Eq. 1 was given in Ref. [1] and also for a single mode in [5] we give a re-derivation of it here for completeness. For simplicity we will perform the derivation in the absence of loss. The inclusion of loss is quite straightforward.

We begin with the telegrapher's equation for a waveguide. Treating the system as a string of coupled inductors and capacitors we have the constitutive equations

$$\partial_x I = -\mathcal{C} \partial_t \mathcal{V} \quad (\text{S1})$$

$$\partial_x \mathcal{V} = -\mathcal{L} \partial_t I \quad (\text{S2})$$

where  $\mathcal{V}$  is the electrostatic potential, and  $I$  is the current. Here  $\mathcal{C}$  is the capacitance per unit length and  $\mathcal{L}$  is the inductance per unit length. One can view the system as being made of discrete elements separated by distance  $a$ , with  $\mathcal{L}a$  and  $\mathcal{C}a$  the inductance and capacitance of each individual element.

The boundary conditions for a half-wave cavity of length  $\ell$  are  $I(x=0) = I(x=\ell) = 0$  and correspondingly  $\partial_x \mathcal{V}(x=0) = \partial_x \mathcal{V}(x=\ell) = 0$ . Given these boundary conditions, we can write

$$I = \sum_{n>0} I_n(t) \sin(2\pi n x / \ell) \quad (\text{S3})$$

$$\mathcal{V} = \sum_{n>0} \mathcal{V}_n(t) \cos(2\pi n x / \ell) \quad (\text{S4})$$

We now couple in the Josephson junction at position  $x_i$ . This injects current  $I_{in} = E_j \sin(\varphi)$  at position  $x_i$  where  $\varphi$  is the phase across the junction (which we will determine later) and we have set  $2e/\hbar = 1$  as before. Due to this current injection, we modify Eq. S1 to read

$$\partial_x I = -\mathcal{C} \partial_t \mathcal{V} + I_{in}(\varphi) \delta(x - x_i) \quad (\text{S5})$$

We can then decompose Eqns. S5 and S2 into spatial Fourier modes giving (for  $m > 0$ )

$$(2\pi m) I_m = -C \partial_t \mathcal{V}_m + 2 \cos(2\pi m x_i / \ell) I_{in}(\varphi) \quad (\text{S6})$$

$$(2\pi m) \mathcal{V}_m = L \partial_t I_m \quad (\text{S7})$$

where  $C = \mathcal{C}\ell$  is the total capacitance and  $L = \mathcal{L}\ell$  the total inductance. Defining

$$\phi_m = \int_{-\infty}^t \mathcal{V}_m(t') dt'$$

we have Eq. S7 written as

$$I_m = 2\pi m \phi_m / L$$

which we plug into Eq. S6 to obtain

$$\frac{(2\pi m)^2}{L} \phi_m = -C \partial_t^2 \phi_m + 2\alpha_m I_{in}(\varphi) \quad (\text{S8})$$

where we have defined

$$\alpha_m = \cos(2\pi m x_i / \ell). \quad (\text{S9})$$

In the experiment, the injection point  $x_i$  is very close to the end of the cavity so  $\alpha_m \approx 1$  for  $m$  not too large. However, there is no reason not to consider the more general case.

Looking also at the voltage at the injection point we have

$$\mathcal{V}(x_{in}) = \sum_{m \geq 0} \alpha_m \mathcal{V}_m$$

The waveguide is DC-biased using the technique of Ref. [4], which couples to the  $\mathcal{V}_0$  mode which we then identify as the applied voltage  $V$ . We thus have

$$\varphi(t) = \int_{-\infty}^t dt' \mathcal{V}(x_{in}, t') = Vt + \sum_{m>0} \alpha_m \phi_m(t)$$

Plugging this into Eq. S8 obtains our final result Eq. 1, except for the loss term which we have dropped only for convenience of notation here.

### Supp. 2: The Green's Function

Given a damped harmonic oscillator with a  $\delta$  function source

$$\ddot{\phi} = -\omega^2 \phi - 2\gamma \dot{\phi} + \delta(t), \quad (\text{S10})$$

it is easy to show that the response is

$$G(t) = \frac{e^{-\gamma t} \sin \tilde{\omega} t}{\tilde{\omega}} \Theta(t)$$

where

$$\tilde{\omega} = \sqrt{\omega^2 - \gamma^2}.$$

Now defining

$$\Psi = \sum_n \alpha_n \phi_n$$

we get a response function for  $\Psi$  given by

$$K(t) = \sum_n \alpha_n^2 \frac{e^{-\gamma t} \sin \tilde{\omega}_n t}{\tilde{\omega}_n} \Theta(t). \quad (\text{S11})$$

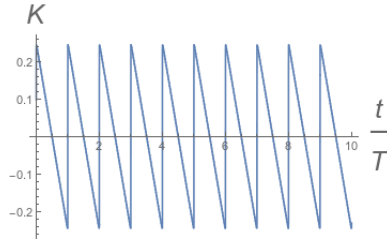


FIG. S1. This is the ideal sawtooth  $K^0$  with  $\alpha_n = 1$  and  $\omega_n = n\omega_0$  and no loss,  $\gamma = 0$ .

For the simplest case discussed in the text ( $\alpha_n = 1$ ,  $\gamma = 0$ ), the form of  $K$  is a simple sawtooth as shown in Fig. S1.

In the case where couplings  $\alpha_n$  have some randomness, it is important to point out that the periodicity remains strictly  $T$ , although the waveform changes. Nonetheless, as shown in Fig. S2 the sharp step rise remains quite robust. If  $\alpha_n$  is smoothly cut off above some scale of  $n$

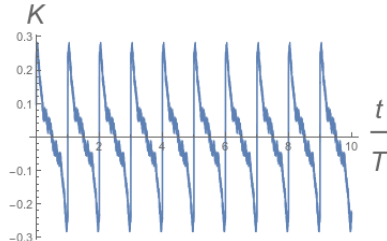


FIG. S2. This is  $K(t)$  if  $\alpha_n$  is chosen randomly between .8 and 1.2 and  $\gamma = 0$ . Notice that the step features remain robust, and the periodicity is fully maintained.

(which appears to be what was used in the simulation of Ref. [1]), then the form of  $K$  will be smooth, and the slope of the step will be limited by the cutoff. A more physical situation is given by  $\alpha_n$  given by Eq. S9 corresponding to the Josephson junction not being positioned quite at the end of the cavity. In this case there will be peaks in  $K(t)$  corresponding to the reflection times from either end of the cavity. An example of this is shown in Fig. S3. The sawtooth response of  $\Psi$  will reflect these multiple steps.

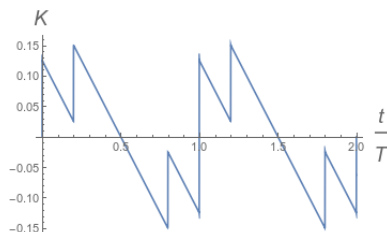


FIG. S3. This is  $K(t)$  if  $\alpha_n$  is given by Eq. S9 with the injection point being at  $x_i = .1l$  and  $\gamma = 0$ . The multiple steps correspond to the time delays given by the round trip times to either end of the cavity.

In the case with  $\gamma$  nonzero, as mentioned in the text a very good approximation is to take  $K(t) = e^{-\gamma t} K^0(t)$ . The difference between this form and the actual calculated  $K$  is due to the difference between  $n\omega_n = n\omega_0$  and  $\tilde{\omega}_n$  which is tiny. Strictly speaking the difference is order  $\gamma^2$  but plotting the two different functions for  $\gamma$  even as large as unity, they are essentially indistinguishable.

Adding randomness to the frequencies  $\omega_n$  does have a strong effect on  $K$  as shown in Fig. S4, although the sharp step remains a robust feature.

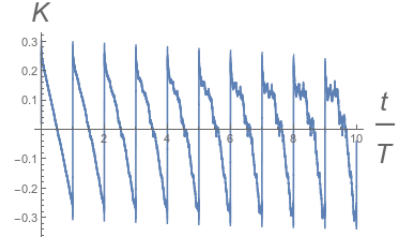


FIG. S4. This is  $K(t)$  if  $\omega_n$  is chosen randomly between  $(n - .05)\omega_0$  and  $(n + .05)\omega_0$  and  $\gamma = 0$ . While the step features remain robust, the periodicity is slowly destroyed.

### Supp. 3: Numerical Results For Parameters Close to That of Experiment

The parameters chosen for the figures in the main text are used mainly for clarity of presentation and to elucidate some of the physics that can occur. (Note that as mentioned in the main text, with nonlinear equations, multiple types of solutions may be possible.) Much of the physics we discuss in the main text is also observed in the more experimentally relevant parameter regime. In the experiment of Cassidy *et al.* [1] the voltage range of lasing is between  $V = 6\omega_0 - 16\omega_0$ . The  $Q$ -factor is stated as roughly 1000, so  $\gamma = 0.0005$  since  $Q = \omega_0/(2\gamma)$ . The coupling constant is estimated as  $\lambda \gtrsim 1$  in units where  $T = 2\pi$ . We take  $\lambda = 3$  as an example.

With units of  $T = 2\pi$  or  $\omega_0 = 1$ , we start by looking at a commensurate case of  $V = 12$  in Fig. S5. Here again we see the characteristic sawtooth shape analogous to that of Fig. 1. Note however, that the sawtooth here is not perfect.

Other solutions to the nonlinear equation, which are even less sawtooth-like, may also appear as shown in Fig. S6. Again there is still some sawtooth-like behavior, and clearly some periodicity, although obviously the signal is more complex.

Moving slightly away from commensuration with  $V = 12.01$  we see in Fig. S7 much of the same features as we have in Fig. 2 in the main text. Note that here the slope is very slightly different from prediction, but otherwise seems to fit well and as with the main text  $\langle \Psi \rangle$  and  $\langle \sin \beta \rangle$  overlay exactly on top of each other. Note that there are

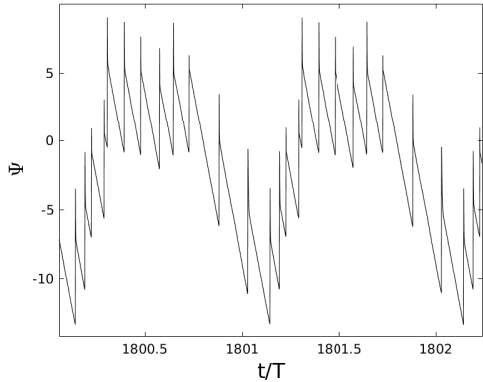


FIG. S5. Pattern of  $\Psi$  for commensurate voltage with parameters close to that of the experiment. With units where  $T = 2\pi$  we use  $\lambda = 3$  with  $\gamma = .0005$  and commensurate driving  $V = 12.0$ . The sawtooth structure is evident although not perfect.

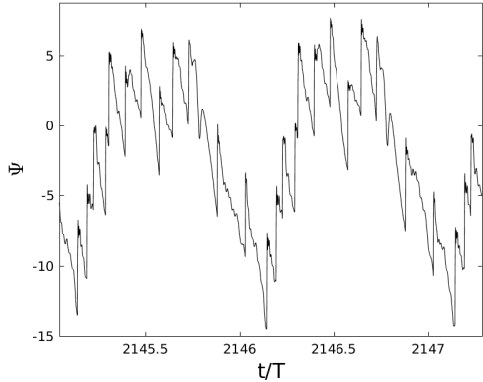


FIG. S6. Pattern of  $\Psi$  for commensurate voltage with parameters close to that of the experiment. With units where  $T = 2\pi$ , we use  $\lambda = 3$  with  $\gamma = .0005$  and commensurate driving  $V = 12.0$ .

some imperfections in the periodicity of the oscillations in the top half of the figure.

Moving slightly further away from commensuration with  $V = 12.1$  we see in Fig. S8 much of the same features as we have in Fig. 2 in the main text and as in Fig. S7 although the pattern is more complicated with a higher number of regions where the quasiperiodicity is lost. Note that in the lower half of this figure one can discern the two separate curves for  $\langle \Psi \rangle$  and  $\langle \sin \beta \rangle$  although they overlap very closely. Note that the average of  $\langle \sin \beta \rangle$  does not strike  $-1$  before the pattern makes a jump here.

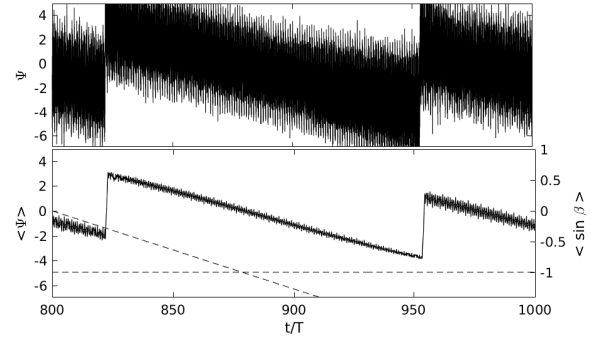


FIG. S7. Pattern of  $\Psi$  for commensurate voltage with parameters close to that of the experiment. With units where  $T = 2\pi$ , we use  $\lambda = 3$  with  $\gamma = .0005$  and voltage  $V = 12.01$ . In the lower half, as in Fig. 2b of the main text, the plot of  $\langle \Psi \rangle$  and  $\langle \sin \beta \rangle$  overlap so you cannot distinguish the two curves.

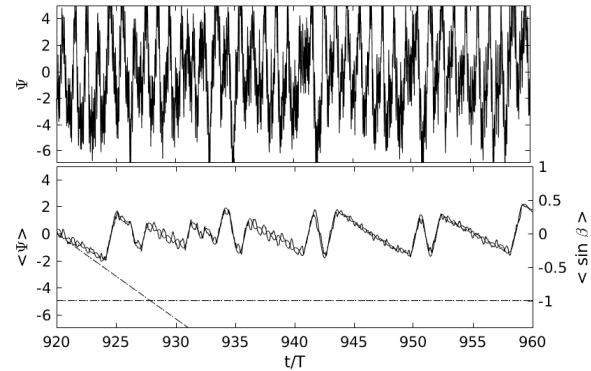


FIG. S8. Pattern of  $\Psi$  for commensurate voltage with parameters close to that of the experiment. With units where  $T = 2\pi$ , we use  $\lambda = 3$  with  $\gamma = .0005$  and voltage  $V = 12.1$ .